

Orbital phase transition in 2-d pyrochlore

Abhinav Saket¹ and Rajarshi Tiwari²

¹*Harish Chandra Research Institute, Chhatnag Road, Jhansi Allahabad, India and*

²*School of Physics and CRANN, Trinity College, Dublin 2, Ireland*

(Dated: September 8, 2018)

We present here correlation driven orbital Mott transition in 2 dimensional pyrochlore lattice. We study a model Hamiltonian in which we take Hund's coupling between itinerant and localized electrons apart from the coulomb interaction. In the weak coupling limit, we calculate zero temperature susceptibility under random phase approximation and find the model in para orbital phase. In strong coupling limit, we calculate the effective Hamiltonian using Green function perturbation theory and find out ferro-orbital ordering at zero temperature. Finally, we use a static auxiliary field based Monte Carlo, explicitly retaining all the spatial correlations, to study finite temperature phase diagram of the model.

PACS numbers: 71.30+h, 71.27+a

I. INTRODUCTION

Since last 25 years, there has been an explosion of interest in the magnetic behavior of pyrochlore oxides. They exhibit metallic, insulating or semi-conducting behavior often coupled with magnetic phase transitions. Pyrochlores are a good system for studying the effects of spin-orbital interplay. A main goal is to understand how various phase transition such as magnetic ordering and metal insulator transitions emerges from this interplay. Most importantly, pyrochlores provide an opportunity to study the role of geometrical frustration in phase transitions.¹ The metal-insulator transition (MIT) in Mo pyrochlore oxides ($R_2Mo_2O_7$) (where R is rare earth metal) and role of its frustrated lattice structure has been extensively studied^{7,11}. The evolution of charge dynamics at metal-insulator transition has been spectroscopically investigated for $Nd_2(Ir_{1-x}Rh_x)_2O_7$ where the spin-orbit interaction as well as the electron correlation is effectively tuned by the doping level (x)¹⁰. The transition from ferromagnetic metal to spin glass insulator and paramagnetic metal has been observed with increase of the radius of rare earth metal ion R^{3+} and external pressure due to the competing double exchange and super exchange interactions on the frustrated lattice¹³.

Compounds with B=Mn, Mo, Ir and Os are interesting as they undergo metal-insulator transition (MIT) by changing temperature, pressure and R-site cations. For example, Coulomb interactions has been found important for MIT and giant magnetoresistance for systems with 3d electrons like B=Mn^{2,3}. On the other hand, for 5d systems with B=Ir and Os, recent first-principles studies revealed that spin-orbit interaction plays a major role in their electronic and magnetic properties^{4,5}. In these systems the natural tendency to form long-range ordered ground states is frustrated, resulting in some novel short-range ordered phases like spin glasses⁶, spin ices, and spin liquids. The role of Orbital degrees of freedom has been proposed in metal insulator transitions in various pyrochlore oxides⁸. In this work, we focus on phase transition in orbital degrees of freedom in pyrochlore.

II. MODEL HAMILTONIAN

The lattice structure of $R_2Mo_2O_7$ is composed of two intervening pyrochlore lattices formed by Mo cations and R cations. In this work, we neglect the coupling between Mo 4d electrons and R site rare earth metal moments and focus on Mo pyrochlore network alone.¹⁷ In Mo pyrochlore lattice, the Mo cation is surrounded by octahedra of oxygens (MoO_6). The octahedral crystal fields of oxygen splits five fold degenerate d orbitals of Mo cation into lower three fold degenerate t_{2g} and higher two fold degenerate e_g levels. Further, the MoO_6 octahedron is distorted along the direction toward the center of each Mo tetrahedron, also known as the local (111) axis or trigonal axis. The distortion in the MoO_6 octahedron along trigonal axis splits three fold t_{2g} level into lower singlet a_{1g} level (below the Fermi level) and higher two fold degenerate e'_g levels (above Fermi level)¹². Mo electronic configuration is Kr $4d^55s^1$. As there are only two electrons in outermost d shell of Mo^{4+} cation, the singlet a_{1g} up spin band (Formation of up spin channel and down spin channel happens because of strong Hund's coupling.) is fully occupied and the two fold degenerate upper e'_g up spin band is half occupied. Since these e'_g electrons reside in a half filled band above Fermi level, they hop from site to site with two fold degeneracy at each site and contribute in conductance. On the other hand, a_{1g} electrons are sitting in a fully occupied band below the Fermi level. They act like spin half localized spins interacting with each other via anti-ferromagnetic super exchange mechanism and play a role in shaping the overall phase competition. On pyrochlore lattice, these a_{1g} and e'_g electrons compete to produce a resultant order. In addition, the itinerant electrons and localized spin half electrons interact via ferromagnetic Hund's rule coupling or double exchange mechanism. The model we study in this paper takes all these into account including on-site coulomb interaction between degenerate e'_g electrons.

We start with the two band orbital double exchange (DE) model Hamiltonian previously proposed for various pyrochlore systems¹⁴⁻¹⁶ that includes kinetic en-

ergy, coulomb interaction, Hund's coupling and anti-ferromagnetic super-exchange,

$$\begin{aligned}
H = & - \sum_{\langle ij \rangle, \alpha, \beta, \sigma} t_{\alpha, \beta} \left(c_{i, \alpha, \sigma}^\dagger c_{j, \beta, \sigma} + h.c \right) \\
& + J_H \sum_{i, \alpha, r, s} c_{i, \alpha, r}^\dagger \vec{\sigma}_{r, s} c_{i, \alpha, s} \cdot \vec{S}_i + J_{AF} \sum_{\langle ij \rangle} \vec{S}_i \cdot \vec{S}_j \\
& + \sum_{i, \alpha, \beta, \alpha', \beta', \sigma, \sigma'} U_{\alpha, \beta, \alpha', \beta'} c_{i, \alpha, \sigma}^\dagger c_{i, \beta, \sigma'}^\dagger c_{i, \beta', \sigma'} c_{i, \alpha', \sigma}
\end{aligned} \quad (1)$$

The first term denotes kinetic energy of itinerant e'_g electrons with spin σ and with orbital index α running over degenerate orbitals a and b of the e'_g band. Second term, J_H , denotes the Hund's coupling between itinerant e'_g electrons with localized spin half a_{1g} electron. Third term, J_{AF} , denotes the anti ferromagnetic super-exchange (SE) among localized a_{1g} electrons. J_{AF} is approximately set by $t_{a_{1g}}^2/U_{a_{1g}}$ where $t_{a_{1g}}$ is the transfer integral between the a_{1g} orbitals and $U_{a_{1g}}$ the intra-orbital Coulomb repulsion in the a_{1g} orbital. The last term denotes on-site coulomb interactions between e'_g including intra and inter-orbital repulsions.

The pressure-induced lattice contraction leads to the increase of the electron transfer interactions. In contrast to the chemical pressure with the R-ion size variation in which the e_g transfer (t) is most effectively modified, the isotropic lattice contraction by the physical pressure act on the a_{1g} electrons, enhancing the antiferromagnetic SE interaction (J_{AF}) between the localized a_{1g} electron spin^{13,17}.

We study two band DE model (1) on the two dimensional checkerboard lattice in the limit $J_{AF} = 0$. We take this lattice because checkerboard lattice has frustrated lattice structure like pyrochlore lattice but has simpler two band Hamiltonian. The checkerboard lattice is shown in fig.1.

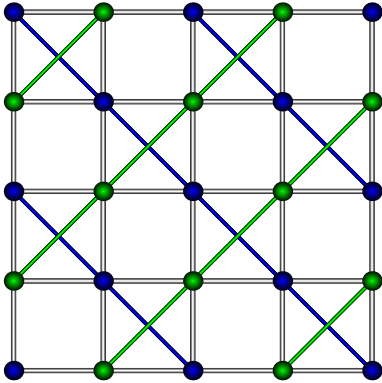


FIG. 1: The checkerboard lattice. The blue and green bonds are for visual distinction only, we take hopping on all the bonds to be the same.

For large J_H , we can simplify the model. We first rotate the axis of quantization of every fermionic operator

$c_{i, \alpha}$ from universal z-axis to the direction of the core spin $\vec{S}_i(\theta_i, \phi_i)$ at every site by transformation,

$$\begin{bmatrix} c_{i, \uparrow} \\ c_{i, \downarrow} \end{bmatrix} = U(\theta_i, \phi_i) \begin{bmatrix} p_i \\ a_i \end{bmatrix}, \quad \text{where} \quad (2)$$

$$U(\theta_i, \phi_i) = \exp\left(-i\frac{\phi_i}{2}\sigma^z\right)\exp\left(-i\frac{\theta_i}{2}\sigma^y\right). \quad (3)$$

This renders the Hund's term diagonal in spin, and in $J_H \rightarrow \infty$ limit, the anti-parallel state gets projected out from the Hamiltonian, the on site energy gets shifted by J_H and we get the spins of itinerant electrons aligned parallel to the localized spin at each site¹⁷.

$$\begin{aligned}
H = & - \sum_{\langle ij \rangle} \sum_{\alpha, \beta} t_{i, \alpha, j, \beta} \left(p_{i, \alpha}^\dagger p_{j, \beta} + h.c \right) \\
& + U \sum_i \sum_{\alpha \neq \beta} n_{i, \alpha} n_{i, \beta}
\end{aligned} \quad (4)$$

where $p_{i, \alpha}$ is spinless fermion operator and $n_{i, \alpha} = p_{i, \alpha}^\dagger p_{i, \alpha}$. In above Eq.(4), U is considered as an inter-orbital interaction and the electronic hopping element $t_{i, \alpha, j, \beta}$ is given by

$$t_{i, \alpha, j, \beta} = t_{\alpha, \beta} \left(\cos \frac{\theta_i}{2} \cos \frac{\theta_j}{2} + e^{i(\phi_i - \phi_j)} \sin \frac{\theta_i}{2} \sin \frac{\theta_j}{2} \right), \quad (5)$$

where (θ_i, ϕ_i) denotes the angle of spin \vec{S}_i , making the hopping element site and spin dependent.

Because of anisotropy of the e'_g orbitals and relative angle of Mo-O-Mo bond¹⁸, the relative strength of $t_{\alpha=\beta}$ and $t_{\alpha \neq \beta}$ can be expressed as

$$\frac{t_{\alpha \neq \beta}}{t_{\alpha = \beta}} = \frac{3 - \cos \delta}{3 + \cos \delta}. \quad (6)$$

In Mo pyrochlore oxides $\delta > 90^\circ$, which means that inter orbital hopping $t_{\alpha \neq \beta}$ is significantly larger than the intra orbital hopping $t_{\alpha = \beta}$ ¹⁷. For simplicity, we neglect the intra orbital hopping $t_{\alpha = \beta} = 0$, and set $t_{\alpha \neq \beta} = t$ and get,

$$\begin{aligned}
H = & - \sum_{\langle ij \rangle} t_{i, j} \left(p_{i, \uparrow}^\dagger p_{j, \downarrow} + p_{i, \downarrow}^\dagger p_{j, \uparrow} + h.c \right) \\
& + U \sum_i n_{i, \uparrow} n_{i, \downarrow}.
\end{aligned} \quad (7)$$

where we replaced orbital degeneracy a, b by spin degeneracy \uparrow, \downarrow and mapped the problem from orbital space to spin space.

III. GROUND STATE

Using Eq.(7), we can find the ground state of the model simply because spin variables \vec{S}_i, \vec{S}_j in hopping amplitude $t_{i, j}$ are decoupled and the energy of electrons in the model can be minimized by simply maximizing $t_{i, j}$. For $t_{i, j}$ to

be maximum, nearest neighboring spins have to be parallel to each other. In parallel spin configuration, the hopping amplitude $t_{i,j}$ becomes site and spin independent. We now study the nature of ground state phases of the model eqn.(7) in extreme limits $t \gg U$ and $t \ll U$. We would give an estimate for the transition point at the zero temperature.

A. Weak coupling limit $t \gg U$:

In limit $t \gg U$, to determine the nature of zero temperature phase of the model, we calculate the zero temperature magnetic susceptibility $[\chi(\mathbf{q})]$. (The square bracket denotes the matrix structure of physical quantity under consideration.) Under the random phase approximation, magnetic susceptibility matrix of interacting electron gas

can be expressed in term of tight binding susceptibility matrix $[\chi^0(\mathbf{q})]$,

$$[\chi(\mathbf{q})] = (g\mu_B)^2 [\chi^0(\mathbf{q})] (\mathbb{I} - U[\chi^0(\mathbf{q})])^{-1}. \quad (8)$$

The magnetic susceptibility matrix $[\chi(\mathbf{q})]$ diverges when

$$|\mathbb{I} - U[\chi^0(\mathbf{q})]| = 0. \quad (9)$$

From eqn.(9), we find the minimum value of U at which the magnetic instability sets in. This eqn. also gives the information about the nature of ordering by locating wave-vector ' \mathbf{q} ' at which the determinant in above eqn. becomes zero. To calculate free electron magnetic susceptibility $[\chi^0(\mathbf{q})]$, we take the external magnetic field term as perturbation to tight binding term and use first order perturbation theory to get,

$$\chi_{\alpha\beta}^0(\mathbf{q}) = \sum_{k,\sigma,\sigma',\gamma,\nu,\delta,\mu} \sigma\sigma' U_{\alpha\sigma',\gamma\nu}^{*k+q} U_{\beta\sigma,\gamma\nu}^{k+q} U_{\beta\sigma,\delta\mu}^{*k} U_{\alpha\sigma',\delta\mu}^k \left\{ \frac{\theta(\epsilon_F - \epsilon_{k+q,\gamma\nu}) - \theta(\epsilon_F - \epsilon_{k,\delta\mu})}{\epsilon_{k+q,\gamma\nu} - \epsilon_{k,\delta\mu}} \right\}. \quad (10)$$

where $\epsilon_{k,\alpha,\sigma} = \pm 2t$ and $\pm 2t\{1 + 2\cos(k_x)\cos(k_y)\}$, $U_{\alpha\sigma',\delta\mu}^{k(k+q)}$ is a diagonalizing matrix for tight binding part of the Hamiltonian, α, β are sub-lattice indices of unit cell of the checkerboard lattice, γ, δ are running over the band indices and $\sigma, \sigma', \nu, \mu$ are running over spin indices.

Using eqn.(10), we calculate the susceptibility matrix numerically for all values of ' \mathbf{q} ' and find out the magnetic instability from eqn.(9). We find out the paramagnetic phase in the model and zero temperature transition point has been found at $U/t = 3.6$.

B. Strong coupling limit $t \ll U$:

In this method we write the self-interaction term as,

$$Un_{i,\uparrow\tau}n_{i,\downarrow\tau} = \frac{U}{4}(n_i^2 - \sigma_{iz}^2) = \frac{U}{4}[n_i^2 - (\vec{\sigma}_i \cdot \hat{\Omega}_i)^2] \quad (11)$$

where last identity being valid for spin half fermions. In our scheme, we apply the Hubbard Stratanovich transformation to replace the quadratic self-interaction term with an integral over a linear term^{19,20}. The partition function $Z = Tre^{-\beta H}$, therefore, can be written as

$$Z = \int [D\phi] \int [Dm] \int [D\Omega] \int [Dp^\dagger, Dp] e^{-s}$$

where

$$S = \sum_i \int_0^\beta d\tau \left[\frac{m_{i\tau}^2}{U} + \frac{\phi_{i\tau}^2}{U} + i\phi_{i\tau}n_{i\tau} - m_{i\tau}\hat{\Omega}_{i\tau}\vec{\sigma}_{i\tau} \right] - \int_0^\beta d\tau \sum_{\langle ij \rangle, \alpha} t_{ij} (p_{i,\alpha\tau}^\dagger p_{j,\alpha\tau} + h.c.) + \int_0^\beta d\tau \sum_{i\alpha} (\epsilon_{i\alpha} - \mu)n_{i\alpha\tau} + \int_0^\beta d\tau \sum_{i\alpha} p_{i,\alpha\tau}^\dagger \partial_\tau p_{j,\alpha\tau}$$

We calculate the partition function now using perturbation theory and, then, take the limit $\beta \rightarrow \infty$,

$$Z = \int D\mathbf{m}_i \int [Dp, Dp^\dagger] \left[e^{-\int_0^\beta d\tau (H'_\tau + H_{U\tau})} \right] \quad (12)$$

where $(H'_\tau + H_{U\tau})$ is given by Eq. (14).

We, then, make static field approximation retaining space dependent part and ignoring the time dependent part of Hamiltonian²¹,

$$H = - \sum_{\langle ij \rangle} t_{ij} \left(p_{ia}^\dagger R_i^\dagger R_j p_{jb} \right) + h.c. + \sum_i \frac{\mathbf{m}_i^2 + \phi_i^2}{U} + i\phi_i n_i - \mathbf{m}_i \cdot \vec{\sigma}_i \quad (13)$$

The integral over ϕ_i in the partition function has the maximum value near the saddle point $\phi_i = i\frac{U}{2}\langle n_i \rangle$. At

half filling $\langle n_i \rangle = 1$, the saddle point equation becomes $\phi_i = i\frac{U}{2}$ and ϕ_i is integrated out finally to give the effective Hamiltonian,

$$H_{eff} = - \sum_{i,j,\sigma} t_{ij} p_{i,\sigma}^\dagger p_{j,\sigma} - \frac{U}{2} \sum_i \mathbf{m}_i \cdot \vec{\sigma}_i + \frac{U}{4} \sum_i \mathbf{m}_i^2 \quad (14)$$

We have, thus, mapped the original Hubbard problem to electrons coupled to auxiliary magnetic moments \vec{m}_i .

In strong coupling limit, we rotate locally at each site to a frame pointing along direction of spin at that site,

$$p_{i,\alpha} \rightarrow \gamma_{i,\alpha} = R_{i\tau}^\dagger p_{i,\alpha}. \quad (15)$$

Under this transformation,

$$R_{i\tau}^\dagger \sigma_{i\tau} \hat{\Omega}_{i\tau} R_{i\tau} = \sigma_{z\tau}.$$

We write the transformed Hamiltonian (ignoring time dependent part) as,

$$H_0 = \sum_{ij\alpha} m \frac{U}{2} \gamma_{ij\alpha\uparrow}^\dagger \gamma_{ij\alpha\uparrow} - m \frac{U}{2} \gamma_{ij\alpha\downarrow}^\dagger \gamma_{ij\alpha\downarrow} \quad (16)$$

$$H' = - \sum_{ij} t_{i,j}^{\sigma,\sigma'} (\theta_i, \phi_i, \theta_j, \phi_j) \gamma_{i\sigma}^\dagger \gamma_{j\sigma'}. \quad (17)$$

where indices i and j are running over all the bonds of Checkerboard lattice and

$$t_{i,j}^{\uparrow\uparrow} = -t \left(\cos \frac{\theta_i}{2} \sin \frac{\theta_j}{2} e^{\frac{i}{2}(\phi_i + \phi_j)} + \sin \frac{\theta_i}{2} \cos \frac{\theta_j}{2} e^{-\frac{i}{2}(\phi_i + \phi_j)} \right),$$

$$t_{i,j}^{\downarrow\downarrow} = -t \left(\cos \frac{\theta_i}{2} \cos \frac{\theta_j}{2} e^{-\frac{i}{2}(\phi_i + \phi_j)} - \sin \frac{\theta_i}{2} \sin \frac{\theta_j}{2} e^{\frac{i}{2}(\phi_i + \phi_j)} \right),$$

$$t_{i,j}^{\uparrow\downarrow} = -t \left(\cos \frac{\theta_i}{2} \cos \frac{\theta_j}{2} e^{\frac{i}{2}(\phi_i + \phi_j)} - \sin \frac{\theta_i}{2} \sin \frac{\theta_j}{2} e^{\frac{i}{2}(\phi_i + \phi_j)} \right),$$

$$t_{i,j}^{\downarrow\uparrow} = t \left(\sin \frac{\theta_i}{2} \cos \frac{\theta_j}{2} e^{\frac{i}{2}(\phi_i + \phi_j)} + \sin \frac{\theta_i}{2} \sin \frac{\theta_j}{2} e^{-\frac{i}{2}(\phi_i + \phi_j)} \right).$$

We can now calculate the partition function. The first order correction $\int [Dc, Dc^\dagger] e^{-\int_0^\beta d\tau H_{0\tau}} \int d\tau H'_\tau$ becomes zero (applying Wick's theorem).

The second order correction is given by

$$\int [Dc, Dc^\dagger] e^{-\int_0^\beta d\tau H_{0\tau}} \int d\tau_1 \int d\tau_2 H'_{\tau_1} H'_{\tau_2}. \quad (18)$$

We apply Wick's theorem again here and in the limit $\beta \rightarrow \infty$ get second order correction,

$$E^2 = \sum_{ij} \frac{(|t_{ij}^{\uparrow\downarrow}|^2 + |t_{ij}^{\downarrow\uparrow}|^2)}{U}$$

Therefore, the effective Hamiltonian to second order is given by,

$$H_{eff} = \frac{t^2}{U} \sum_{ij} 1 + \cos \theta_i \cos \theta_j$$

$$- \frac{t^2}{U} \sum_{ij} \sin \theta_i \cos \phi_i \sin \theta_j \cos \phi_j$$

$$+ \frac{t^2}{U} \sum_{ij} \sin \theta_i \sin \phi_i \sin \theta_j \sin \phi_j. \quad (19)$$

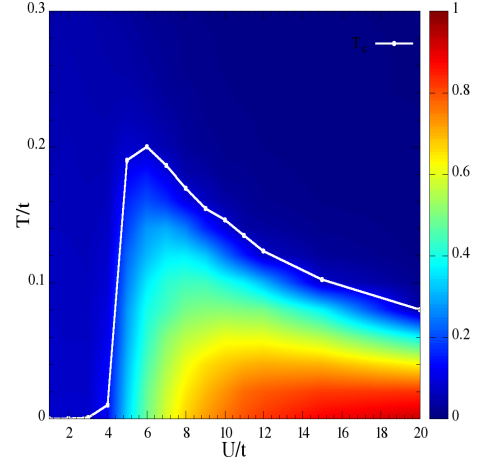


FIG. 2: The phase diagram of the Furukawa model on checkerboard lattice in the $U/t, T/t$ plane. The color map denotes the value of maxima of $S(q)$ at given temperature and U/t . The maxima in this case corresponds to $q=(0,0,0)$, which gives ferromagnetic order. The blue colored regions are where structure factor is very low, or magnetic correlation is very weak to non-existent. The brighter colors like yellow pink and red denote stronger correlations.

which is an anisotropic classical Heisenberg model on checkerboard lattice. Thus, in strong coupling limit, we can find the ground state of the model by Monte Carlo method. We use Metropolis algorithm to implement the Monte Carlo and conclude that the model is a ferromagnet in strong coupling limit.

IV. THERMAL PHYSICS

To access thermal physics, we use Static auxiliary field (SAF) approach earlier used for a comprehensive study of Hubbard model in triangular²², FCC²³ and pyrochlore lattice²⁴.

To calculate the partition function, we use eqn. (14) for all values of U/t . For a given \vec{m}_i configuration, the electron problem is linear and the Hilbert space scales linearly with lattice size. In this work we take the hopping element t_{ij} in eqn. (7) spin and site independent and use a real space Monte-Carlo technique. We start with a configuration of \vec{m}_i with random magnitudes and orientation at high temperature T . We, then, attempt an update $\vec{m}_i \rightarrow \vec{m}'_i$ at site \vec{R}_i . The energy

$$E = -K_B T \ln Tr_{c,c^\dagger} e^{-\beta H_{eff}} \quad (20)$$

is computed before and after the attempted update and $\Delta E = E\{\vec{m}_i\} - E\{\vec{m}'_i\}$ is compared to $k_B T$ in the Metropolis spirit. To calculate the partition function and physical properties at zero temperature, we anneal the sample from higher temperature to zero temperature.

In order to capture the magnetic correlation and transition temperature T_c , we calculate the thermal average

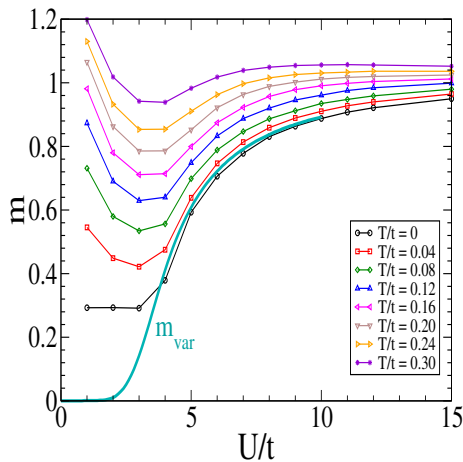


FIG. 3: The average magnetization m and m_{var} as function of U/t at different temperature.

of structure factor defined as

$$S(q) = \frac{1}{N^2} \sum_{ij} \langle \vec{m}_i \vec{m}_j \rangle e^{i\vec{q}(\vec{R}_i - \vec{R}_j)} \quad (21)$$

at each temperature, which serves us as the order parameter of the magnetic transition. We have shown the structure factor $S(q)$ in parameter space of $U/t, T/t$ in fig. (2). At large temperature, $S(q)$ is vanishingly small for all q , however, when lowering the temperature, we notice rapid growth of $S(q)$ at few specific q . The onset

of the growth is shown in the fig. (2) at the magnetic transition temperature T_c as function of U/t .

In fig. (3), we have shown average magnetization versus U/t at various temperature. We observe that average magnetization decreases as temperature increases at given U/t . We have also plotted m_{var} versus U/t which shows dependence of U/t on the magnitude of m_i fields using variational minimizations. Here, we consider an ideal ferro configuration of m_i with magnitude m , and calculate the total energy $E(m)$ as function of m by diagonalizing the Hamiltonian for ferro m_i configuration. Then, $E(m)$ is minimized to find the m_{var} and plotted versus U/t .

V. CONCLUSION

We studied correlation driven orbital Mott transition in 2 dimensional pyrochlore lattice. We studied a model Hamiltonian in which we allow Hund's coupling between itinerant and localized electrons apart from the coulomb interaction. In the weak coupling limit, we calculate the zero temperature orbital magnetic susceptibility under random phase approximation and show that the model exhibits para orbital phase. In strong coupling limit, we calculate the effective Hamiltonian using Green function perturbation theory and establish ferro-orbital ordering at zero temperature. Using static auxiliary field based Monte Carlo, we show finite temperature orbital phase diagram of the model.

-
- ¹ J. S. Gardner, M. J. P. Gingras and J. E. Greedan, Rev. Mod. Phys. **82**, 53 (2010).
 - ² M. A. Subramanian, B. H. Toby, A. P. Ramirez, W. J. Marshall, A. W. Sleight and G. H. Kwei, Science **273**, 81 (1996), <http://www.sciencemag.org/content/273/5271/81.full.pdf>.
 - ³ Y. Shimakawa, Y. Kubo, N. Hamada, J. D. Jorgensen, Z. Hu, S. Short, M. Nohara, and H. Takagi, Phys. Rev. B **59**, 1249 (1999).
 - ⁴ H. Shinaoka, Y. Motome, T. Miyake and S. Ishibashi, Phys. Rev. B **88**, 174422 (2013)
 - ⁵ H. Shinaoka, T. Miyake and S. Ishibashi, Phys. Rev. Lett. **108**, 247204 (2012).
 - ⁶ H. J. Silverstein, K. Fritsch, F. Flicker, A. M. Hallas, J. S. Gardner, Y. Qiu, G. Ehlers, A. T. Savici, Z. Yamani, K. A. Ross, B. D. Gaulin, M. J. P. Gingras, J. A. M. Paddison, K. Foyevtsova, R. Valenti, F. Hawthorne, C. R. Wiebe and H. D. Zhou, Phys. Rev. B **89**, 054433 (2014).
 - ⁷ K. Matsuhira, M. Wakeshima, Y. Hinatsu and S. Takagi, J. Phys. Soc. Jpn. **80**, 094701 (2011).
 - ⁸ N. Hanasaki, K. Watanabe, T. Ohtsuka, I. Kezsmarki, S. Iguchi, S. Miyasaka and Y. Tokura, Phys. Rev. Lett. **99**, 086401 (2007).
 - ⁹ S. Iguchi *et al*, arXiv: 1109.3744v1 [cond-matt.str-el] (2011).
 - ¹⁰ K. Ueda, J. Fujioka, Y. Takahashi, T. Suzuki, S. Ishiwata, Y. Taguchi and Y. Tokura, Phys. Rev. Lett. **109**, 136402 (2012).
 - ¹¹ S. Nakatsuji, Y. Machida, Y. Maeno, T. Tayama, T. Sakakibara, J. vanDuijn, L. Balicas, J.N. Millican, R.T. Macaluso and J.Y. Chan, Phys. Rev. Lett. **96**, 087204 (2006).
 - ¹² I. V. Solovyev, Phys. Rev. B **67**, 174406 (2003).
 - ¹³ S. Iguchi, N. Hanasaki, M. Kinuhara, N. Takeshita, C. Terakura, Y. Taguchi, H. Takagi and Y. Tokura, Phys. Rev. Lett. **102**, 136407 (2009).
 - ¹⁴ Y. Motome and N. Furukawa, Phys. Rev. Lett. **104**, 106407 (2010).
 - ¹⁵ Y. Motome and N. Furukawa, J. Phys.:Conf. Ser. **200** (2010) 012131.
 - ¹⁶ Y. Motome and N. Furukawa, Phys. Rev. B **82**, 060407(R) (2010).
 - ¹⁷ Y. Motome and N. Furukawa, J. Phys.: Conf. Ser. **320** 012060 (2011).
 - ¹⁸ H. Ichikawa *et al*, J. Phys. Soc. Jpn. **74**, 1020 (2005).
 - ¹⁹ H. J. Schulz, Phys. Rev. Lett. **65**, 2462 (1990).
 - ²⁰ J. E. Hirsch, Phys. Rev. B **28**, 4059 (1983).
 - ²¹ T. V. Ramakrishnan and D. Sa
 - ²² R. Tiwari and P. Majumdar, Eur. Phys. Lett. **108** 27007 (2014).
 - ²³ R. Tiwari and P. Majumdar, arXiv:1302.2922 (2013).
 - ²⁴ N. Swain, R. Tiwari and P. Majumdar, arXiv:1505.03502 (2015).